

# Bilateral Descending Hypothalamic Projections to the Spinal Trigeminal Nucleus Caudalis in Rats

Khaled Abdallah, Alain Artola, Lénaïc Monconduit, Radhouane Dallel\*, Philippe Luccarini\*

Clermont Université, Université d'Auvergne, NEURO-DOL: Trigeminal Pain and Migraine, BP 10448, Clermont-Ferrand; Inserm, U1107, Clermont-Ferrand, France

## Abstract

Several lines of evidence suggest that the hypothalamus is involved in trigeminal pain processing. However, the organization of descending hypothalamic projections to the spinal trigeminal nucleus caudalis (Sp5C) remains poorly understood. Microinjections of the retrograde tracer, fluorogold (FG), into the Sp5C, in rats, reveal that five hypothalamic nuclei project to the Sp5C: the paraventricular nucleus, the lateral hypothalamic area, the perifornical hypothalamic area, the A11 nucleus and the retchiasmatic area. Descending hypothalamic projections to the Sp5C are bilateral, except those from the paraventricular nucleus which exhibit a clear ipsilateral predominance. Moreover, the density of retrogradely FG-labeled neurons in the hypothalamus varies according to the dorso-ventral localization of the Sp5C injection site. There are much more labeled neurons after injections into the ventrolateral part of the Sp5C (where ophthalmic afferents project) than after injections into its dorsomedial or intermediate parts (where mandibular and maxillary afferents, respectively, project). These results demonstrate that the organization of descending hypothalamic projections to the spinal dorsal horn and Sp5C are different. Whereas the former are ipsilateral, the latter are bilateral. Moreover, hypothalamic projections to the Sp5C display somatotopy, suggesting that these projections are preferentially involved in the processing of meningeal and cutaneous inputs from the ophthalmic branch of the trigeminal nerve in rats. Therefore, our results suggest that the control of trigeminal and spinal dorsal horn processing of nociceptive information by hypothalamic neurons is different and raise the question of the role of bilateral, rather than unilateral, hypothalamic control.

**Citation:** Abdallah K, Artola A, Monconduit L, Dallel R, Luccarini P (2013) Bilateral Descending Hypothalamic Projections to the Spinal Trigeminal Nucleus Caudalis in Rats. PLoS ONE 8(8): e73022. doi:10.1371/journal.pone.0073022

**Editor:** Izumi Sugihara, Tokyo Medical and Dental University, Japan

**Received:** January 29, 2013; **Accepted:** July 17, 2013; **Published:** August 7, 2013

**Copyright:** © 2013 Abdallah et al. This is an open-access article distributed under the terms of the Creative Commons Attribution License, which permits unrestricted use, distribution, and reproduction in any medium, provided the original author and source are credited.

**Funding:** The work was supported by Institut National de la Santé et de la Recherche Médicale (INSERM), Ministère de l'Enseignement Supérieur et de la Recherche, Université d'Auvergne-Clermont-Ferrand and Région Auvergne. The funders had no role in study design, data collection and analysis, decision to publish, or preparation of the manuscript.

**Competing interests:** The authors have declared that no competing interests exist.

\* E-mail: radhouane.dallel@udamail.fr (RD) Philippe.luccarini@udamail.fr (PL)

## Introduction

Pain is a complex experience that involves sensory-discriminative, cognitive-evaluative, and affective-emotional components. Transmission of nociceptive messages is thus modulated by different central nervous system networks according to the nature of the painful stimulus and behavioral state of the individual [1]. For instance, descending pathways from brainstem and hypothalamus are known to either inhibit or facilitate transmission of nociceptive information at the level of the spinal dorsal horn and the spinal trigeminal nucleus caudalis (Sp5C).

The hypothalamus integrates multiple functions including endocrine and autonomic control, thermoregulation, sleep, appetite, emotional behavior and arousal, and governs the rhythmicity and timing of many body functions [2]. Evidence from neuroimaging studies in man suggest that hypothalamus is also a key player in nociceptive processing, particularly in

trigeminal pain syndromes such as migraine [3] and trigeminal autonomic cephalalgias [4] including cluster headache [5,6]. This prompted the use of deep-brain stimulations to modulate this region in patients with refractory chronic cluster headache [7–10]. Animal studies, using electrophysiological recordings in rats [11–13] and cats [14] or Fos expression as a histochemical marker of neuronal activity [15–17], suggest that the hypothalamus is activated following trigeminal stimulation.

It is widely accepted that trigeminal sensory information can reach the hypothalamus via multisynaptic pathways through the brainstem, thalamus and cortex. Recently, however, anatomical [18–21] and electrophysiological [22] studies showed that a substantial number of Sp5C neurons directly send their axons to hypothalamic regions. The hypothalamus modulates the perception of trigeminal pain [23]. Stimulation or lesion of the A11 nucleus decrease or increase, respectively, dural stimulation-evoked responses of Sp5C neurons [24]. This raises the question as to whether hypothalamic areas directly

project to the Sp5C. To address this issue, we have carried out an anatomical study in the hypothalamus: we microinjected the retrograde tracer, Fluorogold (FG), into Sp5C and looked for retrogradely FG-labeled neurons in hypothalamic nuclei.

## Materials and Methods

Adult male Sprague Dawley rats were obtained from Charles River laboratories (France) and maintained in a light- and temperature controlled environment (lights on 19.00–7.00 h, 22° C) with food and water *ad libitum*. All efforts were made to minimize the number of animals used. The experiments followed the ethical guidelines of the International Association for the Study of Pain [25] and ethical guidelines of the directive 2010/63/UE of the European Parliament and of the Council on the protection of animals used for scientific purposes. Protocols applied in this study have been approved by the local animal experimentation committee: CEMEAA “Comité d’Ethique en Matière d’Expérimentation Animale Auvergne (n° CE 28-12).

### Fluorogold injection

Animals (250–300 g) were anesthetized with chloral hydrate (400 mg/kg body weight, intraperitoneally (i.p.) and placed in a stereotaxic frame. After surgical removing of the atlanto-occipital membrane, glass micropipettes (30–40 µm diameter tips) filled with a 2% solution of Fluorogold (hydroxystilbamidine, Molecular Probes, Reference H22845), diluted in 0.1 M cacodylic acid were positioned at 1–2.4 mm caudal to the obex and inserted into the Sp5C, as lateral on the right as possible (about 2.7 mm), according to Paxinos and Watson [26] with an angle of 80° to the horizontal plane at various depth to reach areas where ophthalmic, maxillary or mandibular primary afferents terminate. The actual position of the iontophoretic injection was verified by recording the extracellular neuronal response to cutaneous mechanical stimulation (brush) of the corresponding dermatome: ophthalmic, maxillary or mandibular. Once the micropipette was in place, direct positive current (5 µA) was applied for 30 s every 30 s for 15–20 min. The microelectrode was left in situ for a further 5 min before withdrawal from the brain. A single injection into the Sp5C was performed in each animal.

Following a postoperative survival period of one week, animals were deeply anaesthetized with urethane (1.5 g/kg i.p) and perfused transcardially over a 15 min period with warm (37 °C) heparinized saline (25 IU heparin/mL) followed by cold (10 °C) phosphate-buffered solution (0.1 M, pH 7.6) containing 4% paraformaldehyde and 0.03% picric acid. The brain and first cervical segment (C1) were removed and then cryoprotected in a buffered 30% sucrose solution containing a paraformaldehyde-picric acid solution and left overnight. Coronal sections were cut on a freezing microtome (40 µm thick) and collected in a 0.05 M Tris-buffered saline (TBS). A set of Sp5C sections was mounted on gelatin-coated slides and viewed using a fluorescent microscope (Zeiss Axioplan 2 Imaging microscope; FG: excitation 365/10 nm, dichroic mirror 400 nm and barrier filter 520 ± 560 nm) in order to localize the injection sites. Only diencephalic sections of animals in which

injection site was exclusively located within the Sp5C were processed further.

### Primary Antibody

A rabbit polyclonal anti-body against Fluorogold (Millipore; Reference AB153; Lot LV1644476) [27] was used in order to detect the retrogradely labeled cells in hypothalamus and the tracer injection site in Sp5C.

### Fluorogold injection site immunocytochemistry

Free-floating brainstem sections were placed in 1% normal horse serum for 30 min before incubation in a rabbit polyclonal antibody directed against Fluorogold (1:20000, Millipore, Reference AB153) overnight at room temperature. Sections were then washed in TBS and placed in biotinylated horse anti-rabbit followed by avidin–biotin–peroxidase complex (Immpress, Abcys Vector, 30 min at room temperature). Immunoreactivity for Fluorogold was visualized in sections using 3,3'-diaminobenzidine tetrahydrochloride (DAB) (kit Vector Peroxidase substrate DAB).

### Hypothalamic section immunocytochemistry

Free-floating diencephalic sections were placed in 1% normal goat serum for 60 min before incubation in a rabbit polyclonal antibody directed against FG (1:20000, Millipore, Reference AB 153) overnight at room temperature. Immunoreactivity was revealed using Cy3 conjugated goat anti-rabbit secondary antibody (1: 200, Jackson Immunoresearch, Reference 111-165-003) for 2 hours at room temperature. All immunolabels were diluted in TBS containing 0.25% bovine serum albumin and 0.3% Triton X-100. Specificity controls consisted of the omission of the primary antibody and incubation of sections in inappropriate secondary antibodies. In all these control experiments, no specific staining was evident. All sections were rinsed in TBS and transferred to gelatinized slides before being coverslipped using DPX.

### Cresyl violet staining

In order to define the cytoarchitecture of paraventricular nucleus (PVN) subdivisions [28–30], a few selected sections were mounted separately and stained with a 0.5% cresyl violet solution for 10 min. Sections were then rinsed with distilled water and dehydrated in graded dilutions of ethanol before being cleared with xylene and coverslipped using DPX.

### Data analysis

Computer-assisted bright-field images of injection sites were obtained using a CCD color video camera (Sony DXC-950P) connected to a Nikon Optiphot-2 microscope at 4× magnification. Each injection site was analyzed using coronal sections processed with DAB. The delineation of the Sp5C was based on our own myeloarchitecture atlas adapted from Strassman and Vos [31] and Molander, et al. [32]. Brainstem sections were categorized according to their approximate rostrocaudal location in the Sp5C (from +0.4 µm to -3.2 µm, 10 levels) relative to the most caudal tip of the subnucleus interpolaris/Sp5C transition region, as described by Yoshida, et

al. [33] which corresponds approximately to obex. Representation of injection sites were grouped on standard drawings of Sp5C. The volumes of injection sites were computed out of their measured rostrocaudal, mediolateral and dorsoventral extents.

Retrogradely labeled neurons were counted in altogether 17 coronal sections throughout the whole antero-posterior extent of hypothalamus. These sections were selected as following. First, every third section from the entire set of microtome sections containing the hypothalamic region was examined with a fluorescence microscope. Sections which appeared to be the closest to the coronal planes -0.9, -1.2, -1.6, -1.8, -1.9, -2.1, -2.3, -2.6, -2.8, -3.1, -3.3, -3.6, -3.8, -4.2, -4.3, -4.5 and -4.8 mm posterior to bregma of the Paxinos and Watson atlas [26] were then selected. In each selected section, immunofluorescence was analyzed with a motorized Zeiss Axioplan 2 Imaging microscope coupled with a Hamamatsu C4742-95 digital camera, by using Texas Red filter set. Images of ipsilateral and contralateral hypothalamic nuclei were captured separately with a x10 objective, resulting in an image size of 1280x1024 pixels. Retrogradely labeled cell bodies within the different hypothalamic nuclei were identified and counted manually with the aid of ImageJ cell counter plugin. The delineation of the hypothalamus was based upon Paxinos and Watson [26], Swanson and Kuypers [28], Skagerberg and Lindvall [34], Cechetto and Saper [29], Swanson, et al. [35]. Representative examples of retrogradely labeled cell bodies distribution were grouped on standard drawings illustrating the rostrocaudal levels of hypothalamus. Images were exported to Adobe PhotoShop (v 5.5) to adjust brightness and contrast before adjusting the image scale by using ImageJ 1.45 software. The images were imported into Coral Draw 12 to insert additional indications and/or anatomical landmarks.

Data in the text, figures and table are expressed as mean  $\pm$  SEM. Statistical analyses were performed using Sigma Plot software. Either the Student *t*-test, Mann-Whitney rank sum test, when data were not normally distributed, and one Way ANOVA followed by *post hoc* Tukey's multiple comparison tests were used as specified in the text. Significance level was set at  $p < 0.05$ .

## Results

### Localization and extent of injection sites

The present data were collected from 21 rats, in which the injection of FG, manifest as a dense core of intense fluorescence, was restricted to Sp5C. The Sp5C localization of FG injections was confirmed by using DAB: each injection appeared as a center of dense FG immunoreactivity surrounded by, first, a halo of staining with strongly FG immunoreactive neurons and then, more peripherally, less stained neurons (Figure 1). Coronal levels at which tracer deposition was maximal were at about -1.2 mm ( $n = 2$ ), -1.6 mm ( $n = 10$ ), -2.0 mm ( $n = 6$ ) and -2.4 mm ( $n = 3$ ) relative to the most caudal tip of the subnucleus interpolaris/Sp5C transition region (Figure 1B). Mean rostrocaudal, mediolateral and dorsoventral extents of injection sites (area of strongly

immunostained neurons) were  $965 \pm 62 \mu\text{m}$ ,  $562 \pm 48 \mu\text{m}$  and  $503 \pm 39 \mu\text{m}$ , respectively.

In most animals ( $n = 15$ ), FG injections were confined to either the dorsomedial ( $n = 3$ ) or intermediate ( $n = 8$ ) or ventrolateral ( $n = 4$ ) area of Sp5C (Figure 1B). These areas are innervated by the mandibular (V3), maxillary (V2) and ophthalmic (V1) branch of the trigeminal nerve (V), respectively. Therefore, it has been possible to also study the organization of hypothalamic projections to each specific Sp5C areas. Representative examples on FG injections into the V3, V2 and V1 areas are illustrated in Figure 1A. In the remaining 6 rats, FG injection were either between the intermediate and ventrolateral areas ( $n = 2$ ) or involved the three areas ( $n = 4$ ).

### Distribution of FG Neurons in the Hypothalamus

FG neurons were predominantly found in the paraventricular nucleus (PVN), lateral hypothalamic area (LH), perifornical hypothalamic area (PFX), A11 nucleus and retrochiasmatic area (RCA) (Figures 2-5). The number of FG neurons was high in the PVN, intermediate in the LH, A11 and PFX, and low in the RCA. Some neurons were scattered throughout the remainder of hypothalamic nuclei.

### FG neurons in the paraventricular nucleus (PVN)

The largest number of descending hypothalamo-trigeminal neurons was observed in the PVN. FG neurons were found in both the ipsilateral and contralateral PVN with nevertheless a clear ipsilateral predominance: the number of FG neurons was much higher in the ipsilateral than in the contralateral PVN (75.5% and 24.5%, respectively of the total number of FG neurons in PVN; Mann-Whitney rank sum test,  $n = 21$ ,  $p < 0.001$ ) (Figures 2B, 3A, 4B).

FG neurons were not uniformly distributed throughout the PVN but mainly restricted to its caudal part, between -1.8 and -2.1 mm posterior to bregma. They were thus preferentially located in some of PVN subdivisions in a pattern that was similar in all investigated animals. The PVN is known to include two clusters of large (magnocellular) and small to medium-sized (parvicellular) neurons [36]. The parvicellular part is subdivided into five subnuclei, the periventricular (pv), anterior (ap), medial (mp), lateral (lp) and dorsal (dp) subdivisions, and the magnocellular part, into three subnuclei, the anterior (am), medial and posterior (pm) groups. FG neurons were concentrated within the lateral and medial parvicellular subdivisions and, less, in the dorsal parvicellular subdivision. Numerous FG neurons were also observed in the posterior magnocellular subdivision (Figure 5, Table 1).

### FG neurons in the lateral hypothalamic area (LH) and perifornical hypothalamic area (PFX)

There were many FG neurons in bilateral LH and PFX (Figures 2C, 2D, 3A, 4C). Whereas, in LH, the number of FG neurons was slightly higher in the ipsilateral than in the contralateral side (63.6 and 36.4%, respectively, of the total number of FG neurons in LH; Mann-Whitney rank sum test,  $n = 21$ ,  $p < 0.001$ ), in PFX, there was no significant difference between the ipsilateral and contralateral sides. FG neurons were observed throughout the LH, between -2.1 and -4.3 mm

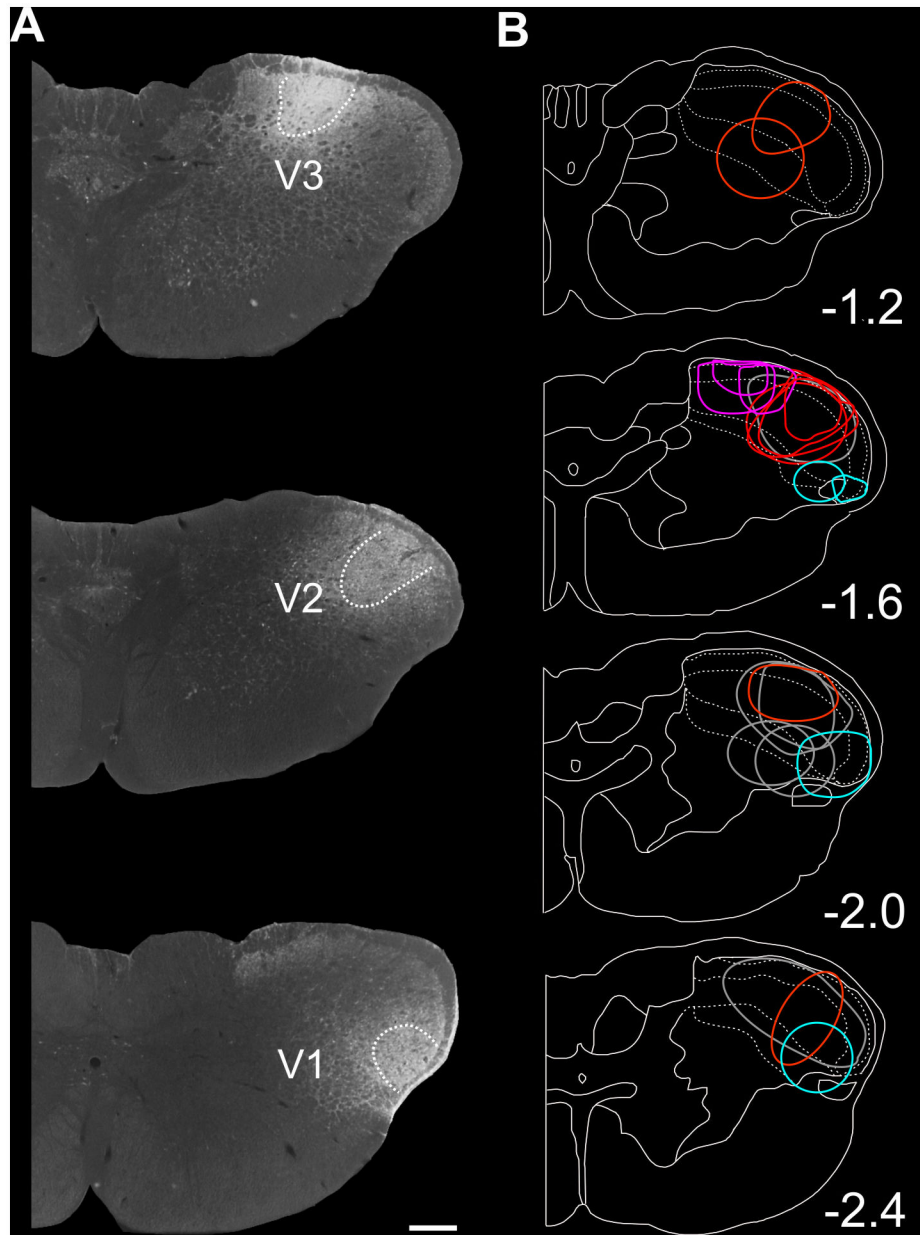


**Figure 1. Localization of Fluorogold (FG) injection sites within the spinal trigeminal nucleus caudalis (Sp5C).** A: Digitized photomicrographs of bulbo-cervical coronal sections showing examples of FG injection sites into the mandibular (V3), maxillary (V2) and ophthalmic (V1) areas of Sp5C; Scale Bar = 300  $\mu$ m. B: Schematic representation illustrating the rostrocaudal distribution of all FG injection sites ( $n = 21$ ) – confined to V1 ( $n = 4$ ; red) V2 ( $n = 8$ ; blue) or V3 ( $n = 3$ ; green) areas or more spread ( $n = 6$ ; grey), from -1.2 to -2.4 mm relative to the most caudal tip of the subnucleus interpolaris/Sp5C transition region and their ventro-dorsal extent within the Sp5C.

doi: 10.1371/journal.pone.0073022.g001

posterior to bregma and in PFX, between -2.8 and -3.6 mm posterior to bregma (Figure 2C, D).

#### FG neurons in the hypothalamic A11 nucleus (A11)

Many FG neurons were also observed in the hypothalamic A11 nucleus (Figures 2E, 3A, 4D). There were slightly more FG

neurons in the contralateral, this time, that in ipsilateral A11 nucleus (58.3 and 41.7% respectively, of the total number of FG neurons in A11; Mann-Whitney rank sum test,  $n = 21$ ,  $p = 0.037$ ). FG neurons were evenly distributed throughout the rostrocaudal extent of the A11 area; that is, in the dorsal and posterior hypothalamus, extending caudally and dorsally along

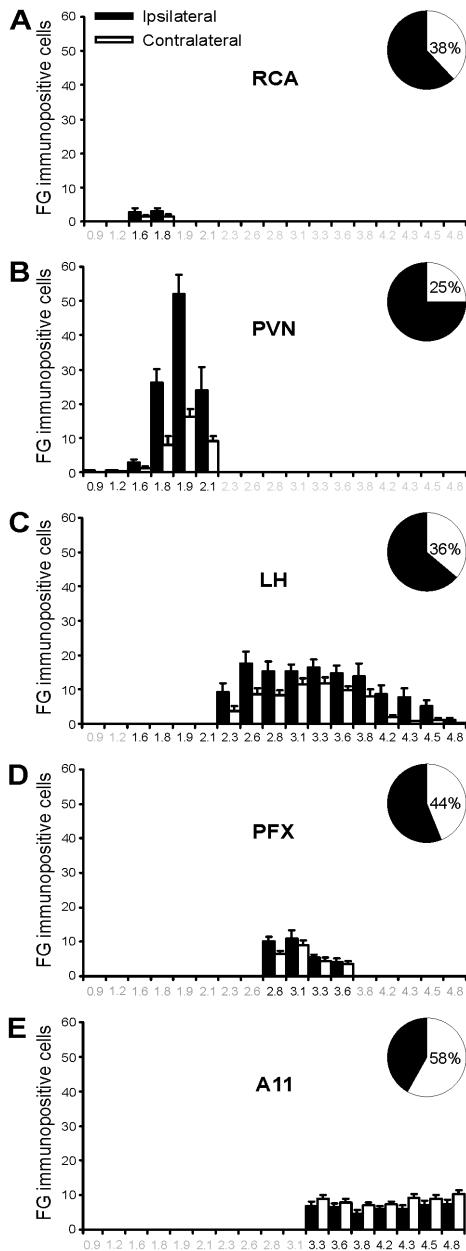


**Figure 2. Rostrocaudal distribution of retrogradely FG-labeled cells in the hypothalamus following FG injections in Sp5C.** A–E: Bar histograms of the number of FG neurons (mean  $\pm$  SEM;  $n = 21$ ) at the ipsilateral (filled bars) and contralateral (empty bars) side on coronal sections plotted as a function of the posterior distance (mm posterior to bregma) within the five hypothalamic nuclei: RCA: retrochiasmatic area (A), PVN: paraventricular nucleus (B), LH: lateral hypothalamus area (C), PFX: perifornical area (D) and A11 (E). Abscissa in black are for the maximum rostrocaudal extent (mm posterior to bregma) of each hypothalamic nucleus: RCA (-1.6 to -1.8 mm), PVN (-0.9 to -2.1 mm), LH (-1.6 to 4.8 mm), PFX (-2.8 to -3.6 mm) and A11 (-3.3 to -4.8 mm). A–E right: Pie charts of the bilateral distribution of FG neurons in each hypothalamic nuclei.

doi: 10.1371/journal.pone.0073022.g002

the periventricular grey of the caudal thalamus, between plans 3.3 to -4.8 mm posterior to bregma [34].

### FG neurons in the retrochiasmatic area (RCA)

The lowest number of descending hypothalamo-trigeminal neurons was in the RCA (Figures 2A, 3A, 4A). There was no lateral predominance. FG neurons were observed between plans -1.6 to -1.8 mm posterior to bregma (Figure 2A).

### Distribution of FG neurons in the hypothalamus as a function of the localization of the injection site

There was no variation in the number of retrogradely FG-labeled neurons according to the rostrocaudal localization of the injection site. On the other hand, the number of retrogradely FG-labeled neurons in the hypothalamus varied with the location of the injection site within Sp5C: V1, V2 or V3. There were many more FG neurons in hypothalamic nuclei following injections into the V1 area of Sp5C than after injections into V2 and V3 areas (One-way ANOVA and *post hoc* Tukey's multiple comparison tests, V1 vs. V2:  $p = 0.004$ , V1 vs. V3:  $p = 0.036$ ,  $n = 15$ ; Figure 6). Moreover, FG neurons could only be observed in RCA following injections in the V1 area: there were no or very few neurons when injections were located in other Sp5C areas (Figure 6). This was not due to larger injections in the V1 area compared with V2 or V3 areas since the volumes of injection sites in V1, V2 and V3 areas ( $0.30 \pm 0.14$ ,  $n=3$ ;  $0.21 \pm 0.28$ ,  $n=8$ ; and  $0.40 \pm 0.14$  mm<sup>3</sup>,  $n=4$ ; respectively) were not different (see Figure 1). Finally, it has been noted that the heaviest hypothalamic projection to the spinal dorsal horn are to lamina I [37]. However, we could not assess the laminar distribution of hypothalamic projections to the Sp5C as most of our Sp5C injections involved all laminae (see Figure 1).

### Discussion

Here, we used the retrograde tracer FG to delineate the organization of hypothalamic projections to the Sp5C. We present the first evidence in rats that mainly five hypothalamic nuclei, the PVN, LH, PFX, A11 and RCA, project to the Sp5C. Hypothalamic projections to Sp5C are bilateral, with, nevertheless, a clear ipsilateral predominance for those originating from the PVN. Interestingly, hypothalamic projections vary between Sp5C areas. The V1 area appears to receive massive hypothalamic projections and it is the only Sp5C area to get inputs from the RCA.

### Technical Considerations

To identify hypothalamic projection neurons, we used Fluorogold, a well-known and effective retrograde tracer [39]. However, the results of this study should be interpreted with the following reservations: (i) though electrophoretic ejections of FG were made small enough to be specific of the V3, V2 and V1 areas of Sp5C, it is possible that some injections had slightly diffused to adjacent Sp5C areas; (ii) since Fluorogold can be taken up and transported by axons of passage [40,41], some of the labeled neurons in the hypothalamus might actually not project to the Sp5C but have their axons passing

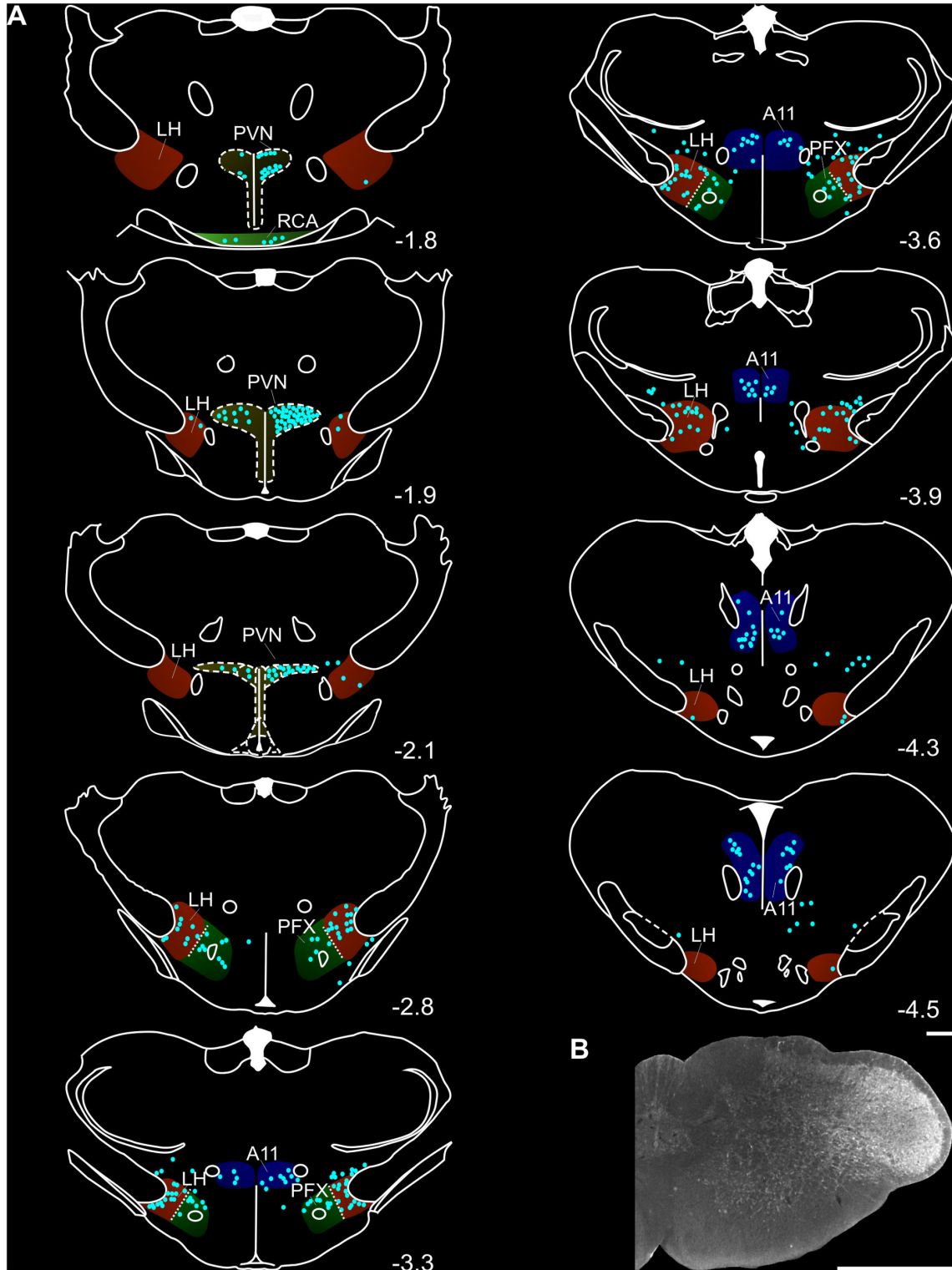


**Figure 3. Rostrocaudal distribution of retrogradely FG-labeled neurons in the hypothalamus after a large FG injection into the Sp5C.** A: Semi-schematic drawings of coronal sections at different levels, from -1.8 to -4.5 mm posterior to bregma. Retrogradely FG-labeled neurons in the hypothalamus and adjacent areas are indicated by red dots. B: A representative injection site of FG in Sp5C. PVN: paraventricular nucleus, RCA: retrochiasmatic area, LH: lateral hypothalamus area, PFX: perifornical area. Scale bar: 300  $\mu$ m.

doi: 10.1371/journal.pone.0073022.g003

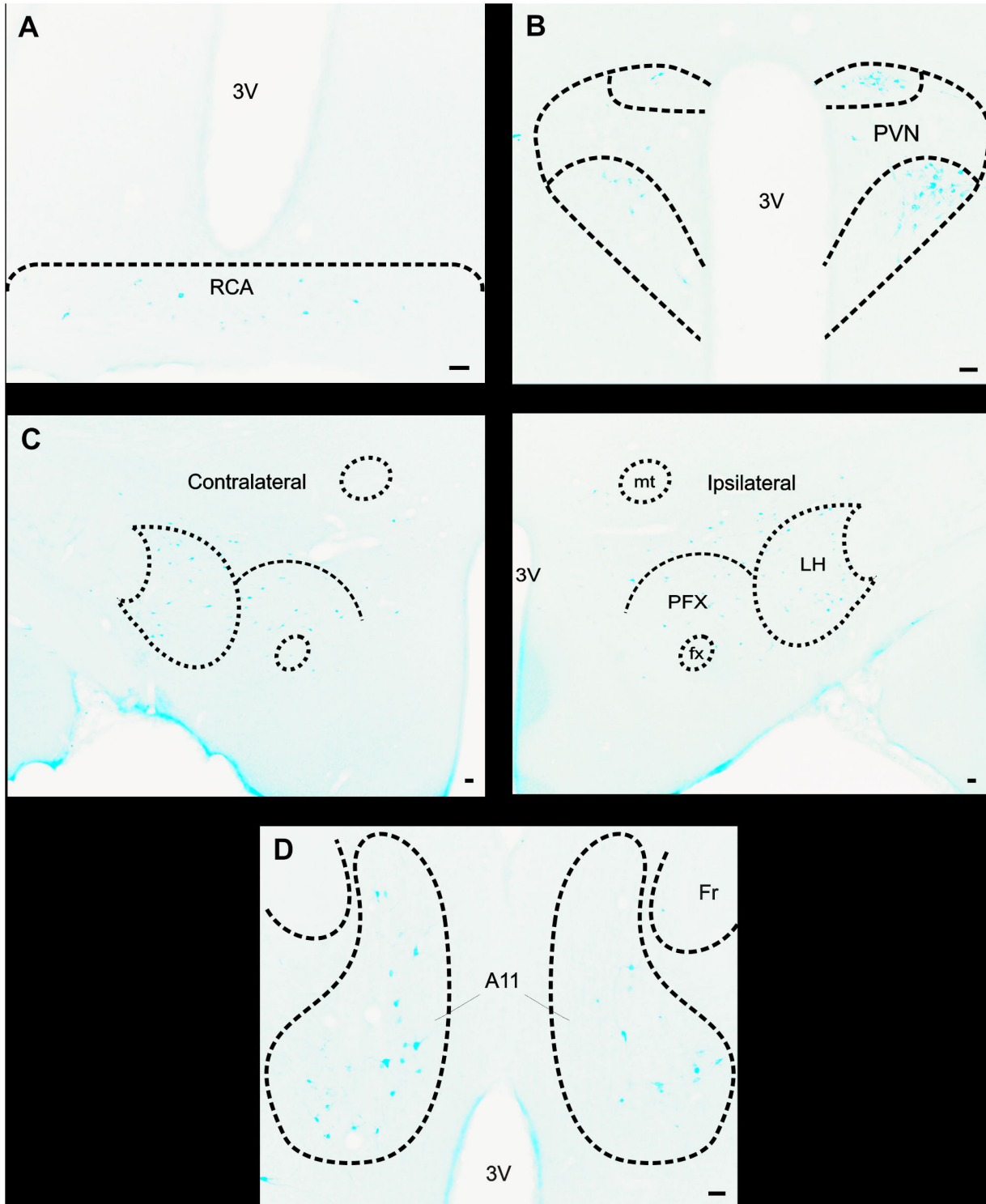


**Figure 4. Examples of retrogradely FG-labeled neurons in the PVN, RCA, LH, PFX and A11 hypothalamic nuclei following a large FG injection into the Sp5C.** A–D: Representative photomicrographs of coronal sections showing retrogradely FG-labeled neurons in the RCA (A), PVN (B), LH and PFX (C) and A11 (D) following a large FG microinjection into the Sp5C (the same as Figure 3). These photomicrographs show clearly that FG-labeled neurons are present on both ipsilateral (on the right in A, B C, and D) and contralateral sides (on the left in A, B C, and D). 3V: third Ventricle, mt: mammillothalamic tract, fx: fornix, Fr: *Fasciculus retroflexus*. Scale bar: 50  $\mu$ m.

doi: 10.1371/journal.pone.0073022.g004

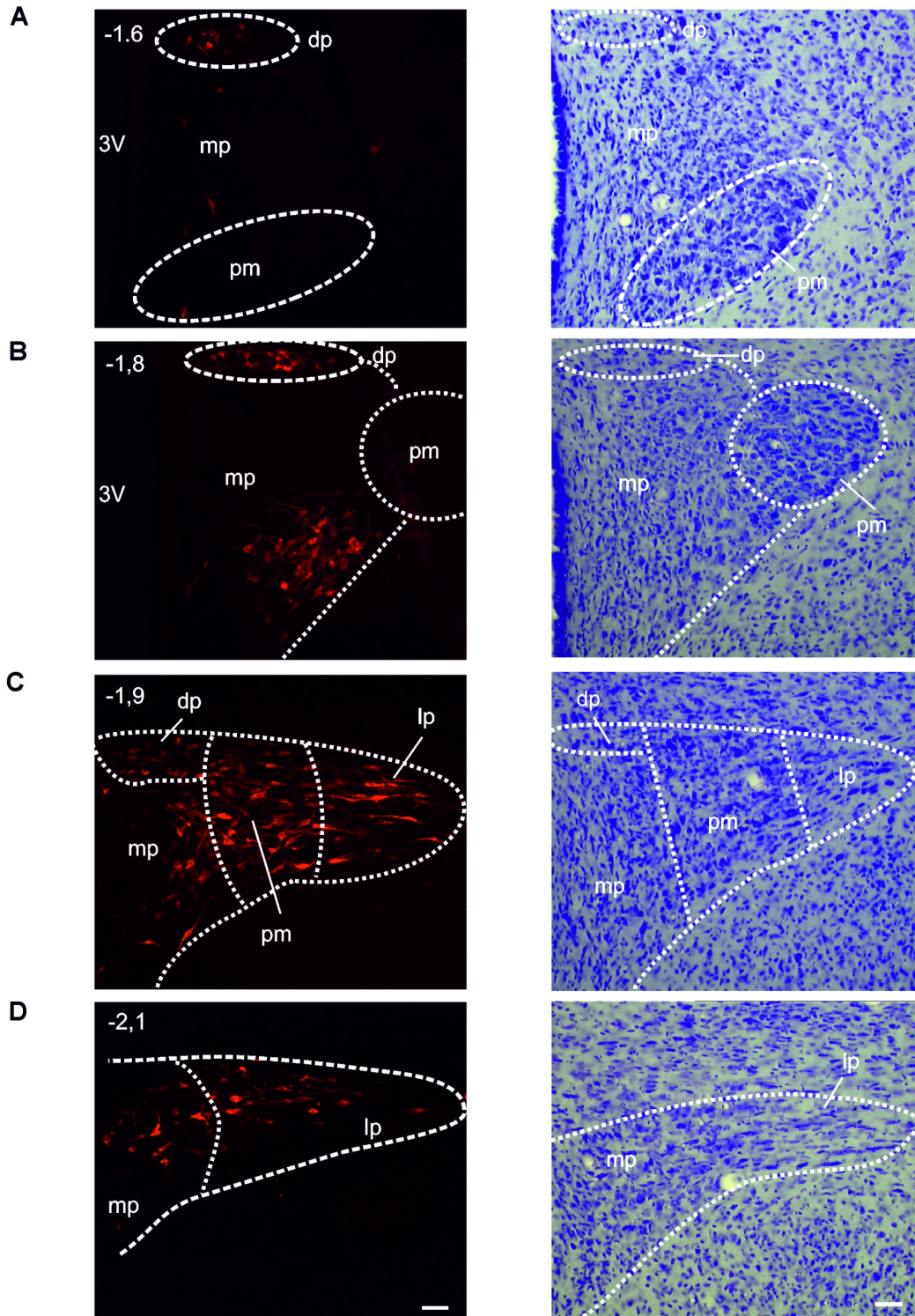


**Figure 5. Example of retrogradely FG-labeled neurons in the ipsilateral PVN following a large FG microinjection into the Sp5C.** A–D: Representative photomicrographs of coronal sections showing the retrogradely labeled neurons (left) and the corresponding cresyl violet stainings (right) through the parvi- and magnocellular PVN at -1.6 (A), -1.8 (B), -1.9 (C) and -2.1 mm (D) posterior to bregma following large FG microinjection into the Sp5C (the same as Figure 3). pv: periventricular part; am: anterior magnocellular part; ap: anterior parvocellular part; lp: lateral parvocellular part; pm: posterior magnocellular part, mp: medial parvocellular part; dp: dorsal parvocellular part of PVN. Scale bar: 50  $\mu$ m.

doi: 10.1371/journal.pone.0073022.g005



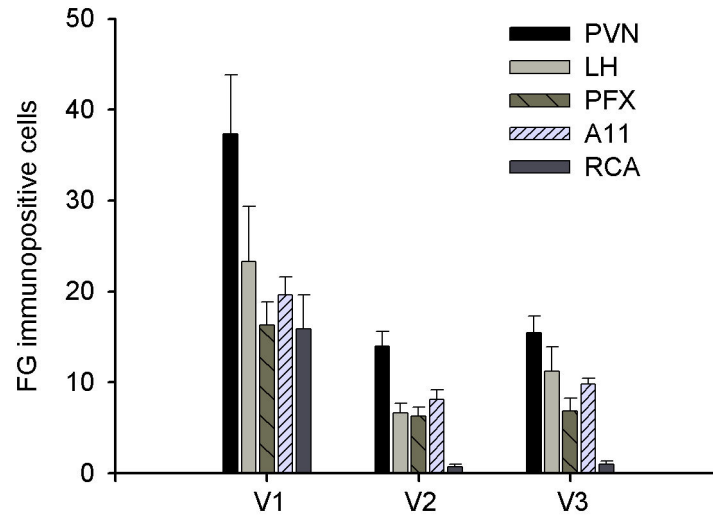


**Figure 6. Distribution of FG neurons in both the ipsilateral and contralateral hypothalamus as a function of the injection site in Sp5C.** Bar histogram of the number of FG neurons (mean number of neurons per section  $\pm$  SEM;  $n = 15$ ) in the five hypothalamic nuclei (PVN, LH, PFX, A11 and RCA) as a function of the localization of the Sp5C injection site: mandibular (V3,  $n=3$ ), maxillary (V2,  $n=8$ ) and ophthalmic (V1,  $n=4$ ) areas.

doi: 10.1371/journal.pone.0073022.g006

**Table 1. Distribution of retrogradely fluorogold labeled neurons within the different subnuclei of parvi- and magnocellular PVN following fluorogold injections into the Sp5C (mean: average number of fluorogold labeled neurons per section; mean  $\pm$  SEM,  $n = 21$ ). ns: non significant.**

PVN subdivisions	Ipsilateral	Contralateral	P values
Anterior parvicellular part	0.5 $\pm$ 0.2	0.1 $\pm$ 0.1	ns
Medial parvicellular part	13.8 $\pm$ 1.9	4.5 $\pm$ 0.9	P<0.001
Dorsal parvicellular part	4.8 $\pm$ 1.0	1.5 $\pm$ 0.5	P<0.01
Lateral parvocellular part	11.7 $\pm$ 2.0	3.4 $\pm$ 0.6	P<0.001
Periventricular part	0.1 $\pm$ 0.1	0.2 $\pm$ 0.2	ns
Anterior magnocellular part	0.0 $\pm$ 0.0	0.0 $\pm$ 0.0	ns
Medial magnocellular part	0.0 $\pm$ 0.0	0.0 $\pm$ 0.0	ns
Posterior magnocellular part	10.7 $\pm$ 1.6	3.7 $\pm$ 0.6	P<0.001

through the injected areas on their way to more caudal spinal cord segments. It has to be noted however that hypothalamic projections to the spinal cord are exclusively ipsilateral [29,36,42]. Therefore, provided that some ipsilateral hypothalamic labeled neurons actually project to the spinal cord, ipsilateral hypothalamic projections to the Sp5C would have been overestimated and conversely contralateral ones underestimated. This would make our conclusion that the organizations of hypothalamic projections to the Sp5C and spinal cord are different even stronger.

#### Anatomical considerations

**The Paraventricular nucleus (PVN).** The projections of magnocellular and parvicellular PVN in rats are different.

Magnocellular neurons project directly to the posterior lobe of the pituitary and parvicellular ones to lower brainstem and spinal cord [29,37–39,42–44]. PVN projections to the spinal cord are mostly ipsilateral.

The present results indicate that PVN also projects directly to the Sp5C. PVN projections to Sp5C are bilateral with, nevertheless, a clear ipsilateral predominance, and, as those to the spinal cord [29,44], originate mainly from the lateral, medial and dorsal subdivisions of parvicellular PVN. Interestingly, a significant number of magnocellular neurons were also retrogradely labeled. Whether magnocellular neurons project to the spinal cord is still a matter of discussion as no [45,46] as well as few [28,47] and significant [30,48,49] magnocellular projections to the spinal cord have been reported. Anyhow, both parvicellular and magnocellular PVN appear to project to the Sp5C. Further studies involving for instance electrophysiological recordings will be needed to determine the actual functional role of such heterogeneous PVN projections to the Sp5C.

**The lateral hypothalamus (LH) and perifornical hypothalamic areas (PFX).** LH and PFX project to other hypothalamic areas as well as to the cortex and spinal cord [2]. Actually, LH and PFX projections to the spinal cord are larger than PVN ones [38]. We show that LH and PFX strongly project to the Sp5C, too. It is interesting to note that, whereas LH and PFX projections to the spinal cord are ipsilateral [38,42,45], those to Sp5C are bilateral with, nevertheless, a slight ipsilateral predominance for LH ones. Using anterograde autoradiographic tracing, Hosoya and Matsushita [50] similarly found sparse labeled fibers in bilateral Sp5C following [ $^3$ H] amino acid injection into LH and PFX.

**The hypothalamus A11 nucleus.** The A11 cell group consists of large neurons that are clustered in the dorsocaudal

region of diencephalon [51]. A11 neurons project primarily to the spinal dorsal horn, with minor projections to the intermediolateral cell column and ventral horn, along the entire spinal cord [52,53]. Our study demonstrates that the A11 nucleus also densely projects to Sp5C. A11 projections to Sp5C are bilateral. This organization is thus different from that of A11 projections to the spinal cord which are predominantly ipsilateral in rats [34], mice [54,55] and monkeys [56].

**The retrochiasmatic hypothalamic area (RCA).** The RCA is constituted of small and medium-sized neurons located just behind the suprachiasmatic nucleus and in front of the arcuate median eminence complex [57]. In addition to thalamic intergeniculate leaflet afferents, the RCA receives projections from the retina, through the retinohypothalamic tract and from the suprachiasmatic nucleus [58–62]. The RCA projects to numerous areas in the central nervous system, including the hypothalamus [63], intergeniculate leaflet [64], and spinal cord [42,43,65]. Our results indicate that RCA also bilaterally projects to Sp5C, but, interestingly, exclusively to the V1 area.

Altogether, our results indicate that the hypothalamic nuclei which send axons to the spinal cord, do also project to the Sp5C. However, the organization of hypothalamic projections to the spinal cord and Sp5C are different: while the former are ipsilateral, the latter are mostly bilateral. Our results show in addition that hypothalamic nuclei do not evenly project to the Sp5C but preferentially to the V1 area, where meningeal and cutaneous inputs from the ophthalmic branch of the trigeminal nerve terminate.

### Functional considerations

Sp5C receives direct inputs from trigeminal primary afferent fibers and contains neurons that respond to noxious and/or innocuous mechanical or thermal stimulations of the cornea [66], temporomandibular joint [67], facial skin [68,69], and intracranial dura [70]. Sp5C neurons are known to directly project to the hypothalamus [18–22]. Together with our evidence for direct hypothalamic projections to the Sp5C, this suggests that connections between the hypothalamus and Sp5C are reciprocal. Hypothalamus might thus be a key element in feedback loops that regulate trigeminal somatosensory inflow. However, whether nociceptive stimuli activate the very hypothalamic neurons that project to Sp5C is still unknown.

**The Paraventricular nucleus (PVN).** In addition to regulating the autonomic nervous system [2], PVN also modulates spinal nociception. Both electrical and chemical stimulation of PVN produce spinal antinociception [71–76], whereas its lesions conversely facilitates nociception [75] and attenuates stress-induced analgesia [71].

Whether PVN also modulates trigeminal nociception is still a matter of discussion. On the one hand, studies using Fos expression have provided inconsistent results. Stimulation of the dura mater has been found to either increase [16] or not change [15,17] Fos expression. And noxious electrical stimulation of tooth pulp fails to enhance Fos expression [77]. But, on the other hand, PVN neurons synthesize and secrete neuropeptides including oxytocin and arginine vasopressin [2]. These peptides are involved in spinal pain processing [78–80]

and also interfere with trigeminal pain. When centrally applied, oxytocin reduces the trigeminal reflex triggered by noxious tooth pulp stimulation [81,82] and, when systemically applied, it attenuates electrical whisker pad stimulation-induced pain-vocalization in newborn rats [83]. Similarly, vasopressin, either centrally applied [81,82] or microinjected into the spinal trigeminal nucleus [84], reduces the amplitude of trigeminal reflex induced by noxious tooth pulp stimulation.

**The lateral hypothalamus area (LH) and perifornical hypothalamic area (PFX).** LH and PFX interfere with spinal cord nociception. For instance, electrical stimulation or microinjection of morphine in LH increases the latency of the tail-flick test [85,86]. And a noxious tooth pulp stimulation activates LH neurons [12,13]. However, it has to be noted that noxious stimulation of the dura mater fails to enhance Fos expression in LH [15–17].

LH and PFX neurons projecting to the spinal cord contain orexin [87,88]. Orexin neurons are primarily known to control sleep and wakefulness, energy metabolism, reward, and addiction [89]. They are also involved in nociception and stress-induced analgesia [90]. The descending orexin system might also modulate trigeminal pain. There is a high density orexin-immunoreactive fibers in superficial Sp5C [87,88]. Interestingly, orexin peptides have been shown to selectively modulate responses to noxious dural but not facial cutaneous stimulation [91]. Together with recent evidence for an association between the orexin receptor 1 gene and migraine [92], this suggests that the orexin system has a specific role in the physiopathology of migraine.

**The hypothalamus A11 nucleus.** The A11 nucleus is involved in the processing of both spinal [91–95] and trigeminal [24] nociceptive information. Direct stimulation and lesion of the A11 nucleus decreases and increases, respectively, the response of Sp5C neurons to dural stimulation [24]. Pain modulation by A11 descending dopaminergic projections is specifically mediated by D2-like receptors [24,93,96]. Directly activating these D2-like receptors inhibits, whereas blocking them enhances, both formalin- and capsaicin-evoked pain behavior as well as C-fiber-evoked action potential firing of trigeminal wide dynamic range (WDR) neurons [96]. Sp5C and spinal dorsal horn both exhibit a strong dopamine labeling, consisting of many varicose fibers, especially in rats and monkeys [53]. Altogether, these results suggest that A11 neurons are the major source of dopamine input to both Sp5C and spinal cord neurons [34].

**The retrochiasmatic hypothalamic area (RCA).** Our results show, for the first time, that RCA projects exclusively to the V1 area. This Sp5C region receives sensory inputs from cranial blood vessels [23] and contains neurons with both dural and peri-ocular receptive fields [70]. RCA projections to Sp5C might thus be specifically involved in the control of migraine pain.

The function of RCA is poorly known. RCA neurons which innervate the spinal cord are alpha melanocyte-stimulating hormone-immunoreactive ( $\alpha$ -MSH) [29]. Alpha-MSH has been shown to interfere with pain [97]. Moreover,  $\alpha$ -MSH neurons in RCA are activated by leptin [65], an adipocyte-derived hormone which decreases body weight. Interestingly,

epidemiologic studies suggest that migraine and chronic daily headache are associated with obesity [98].

## Conclusion

Our results demonstrate that, though hypothalamic projections to the spinal cord and the Sp5C originate from the very same hypothalamic nuclei, the former are ipsilateral whereas the latter are bilateral. Furthermore, these hypothalamic nuclei preferentially, if not exclusively, project to the V1 area. This suggests not only that the hypothalamus differentially modulates trigeminal and spinal somatosensory information but also that it primarily modulates meningeal one. For over 10 years now, hypothalamic stimulation has been used to treat drug-resistant chronic cluster headache with very encouraging results. However, how this stimulation works is not clear and the exact localization of the electrode tip to produce

pain relief still a matter of discussion [8,10]. Therefore, focusing on the organization of hypothalamic projections to the Sp5C is pivotal to get insights into the organization of hypothalamic controls on trigeminal pain, including primary headache disorders.

## Acknowledgements

We thank A.M. Gaydier for secretarial assistance and A. Descheemaeker for technical support.

## Author Contributions

Conceived and designed the experiments: KA AA LM RD PL. Performed the experiments: KA LM PL. Analyzed the data: KA AA LM RD PL. Wrote the manuscript: KA AA RD.

## References

- Millan MJ (2002) Descending control of pain. *Prog Neurobiol* 66: 355-474. doi:10.1016/S0301-0082(02)00009-6. PubMed: 12034378.
- Saper CB (2012) Hypothalamus. *The Human Nervous System*. Elsevier. pp. 549-572.
- Denuelle M, Fabre N, Payoux P, Chollet F, Geraud G (2007) Hypothalamic activation in spontaneous migraine attacks. *Headache* 47: 1418-1426. PubMed: 18052951.
- Holle D, Katsarava Z, Obermann M (2011) The hypothalamus: specific or nonspecific role in the pathophysiology of trigeminal autonomic cephalalgias? *Curr Pain Headache Rep* 15: 101-107. doi:10.1007/s11916-010-0166-y. PubMed: 21128020.
- May A, Bahra A, Büchel C, Frackowiak RS, Goadsby PJ (1998) Hypothalamic activation in cluster headache attacks. *Lancet* 352: 275-278. doi:10.1016/S0140-6736(98)02470-2. PubMed: 9690407.
- May A, Ashburner J, Büchel C, McGonigle DJ, Friston KJ et al. (1999) Correlation between structural and functional changes in brain in an idiopathic headache syndrome. *Nat Med* 5: 836-838. doi: 10.1038/10561. PubMed: 10395332.
- Leone M, Franzini A, Bussone G (2001) Stereotactic stimulation of posterior hypothalamic gray matter in a patient with intractable cluster headache. *N Engl J Med* 345: 1428-1429. doi:10.1056/NEJM200111083451915. PubMed: 11794190.
- Leone M, Franzini A, Proietti Cecchini A, Bussone G (2013) Success, failure, and putative mechanisms in hypothalamic stimulation for drug-resistant chronic cluster headache. *Pain* 154: 89-94. doi:10.1016/j.pain.2012.09.011. PubMed: 23103434.
- Schoenen J, Di Clemente L, Vandenheede M, Fumal A, De Pasqua V et al. (2005) Hypothalamic stimulation in chronic cluster headache: a pilot study of efficacy and mode of action. *Brain* 128: 940-947. doi: 10.1093/brain/awh411. PubMed: 15689358.
- Fontaine D, Lanteri-Minet M, Ouchchane L, Lazorthes Y, Mertens P et al. (2010) Anatomical location of effective deep brain stimulation electrodes in chronic cluster headache. *Brain* 133: 1214-1223. doi: 10.1093/brain/awq041. PubMed: 20237130.
- Shigenaga Y, Matano S, Okada K, Sakai A (1973) The effects of tooth pulp stimulation in the thalamus and hypothalamus of the rat. *Brain Res* 63: 402-407. doi:10.1016/0006-8993(73)90113-3. PubMed: 4764310.
- Morita N, Tamai Y, Tsujimoto T (1977) Unit responses activated by tooth pulp stimulation in lateral hypothalamic area of rat. *Brain Res* 134: 158-160. doi:10.1016/0006-8993(77)90934-9. PubMed: 912414.
- Hamba M, Hisamitsu H, Muro M (1990) Nociceptive projection from tooth pulp to the lateral hypothalamus in rats. *Brain Res Bull* 25: 355-364. doi:10.1016/0361-9230(90)90220-T.
- Rudomin P, Malliani A, Borlone M, Zanchetti A (1965) Distribution of electrical responses to somatic stimuli in the diencephalon of the cat with special reference to the hypothalamus. *Arch Ital Biol* 103: 60-89. PubMed: 14277248.
- Malick A, Jakubowski M, Elmquist JK, Saper CB, Burstein R (2001) A neurohistochemical blueprint for pain-induced loss of appetite. *Proc Natl Acad Sci U S A* 98: 9930-9935. doi:10.1073/pnas.171616898. PubMed: 11504950.
- Ter Horst GJ, Meijler WJ, Korff J, Kemper RH (2001) Trigeminal nociception-induced cerebral Fos expression in the conscious rat. *Cephalalgia* 21: 963-975. doi:10.1046/j.1468-2982.2001.00285.x. PubMed: 11843868.
- Benjamin L, Levy MJ, Lasalandra MP, Knight YE, Akerman S et al. (2004) Hypothalamic activation after stimulation of the superior sagittal sinus in the cat: a Fos study. *Neurobiol Dis* 16: 500-505. doi:10.1016/j.nbd.2004.03.015. PubMed: 15262261.
- Iwata K, Kenshalo DR Jr., Dubner R, Nahin RL (1992) Diencephalic projections from the superficial and deep laminae of the medullary dorsal horn in the rat. *J Comp Neurol* 321: 404-420. doi:10.1002/cne.903210308. PubMed: 1506477.
- Newman HM, Stevens RT, Apkarian AV (1996) Direct spinal projections to limbic and striatal areas: anterograde transport studies from the upper cervical spinal cord and the cervical enlargement in squirrel monkey and rat. *J Comp Neurol* 365: 640-658. doi:10.1002/(SICI)1096-9861(19960219)365:4. PubMed: 8742308.
- Li JL, Kaneko T, Shigemoto R, Mizuno N (1997) Distribution of trigeminohypothalamic and spinohypothalamic tract neurons displaying substance P receptor-like immunoreactivity in the rat. *J Comp Neurol* 378: 508-521. doi:10.1002/(SICI)1096-9861(19970224)378:4. PubMed: 9034907.
- Malick A, Burstein R (1998) Cells of origin of the trigeminohypothalamic tract in the rat. *J Comp Neurol* 400: 125-144. doi:10.1002/(SICI)1096-9861(19981012)400:1. PubMed: 9762871.
- Malick A, Strassman RM, Burstein R (2000) Trigeminothalamic and reticulohypothalamic tract neurons in the upper cervical spinal cord and caudal medulla of the rat. *J Neurophysiol* 84: 2078-2112. PubMed: 11024099.
- Akerman S, Holland PR, Goadsby PJ (2011) Diencephalic and brainstem mechanisms in migraine. *Nat Rev Neurosci* 12: 570-584. doi: 10.1038/nrn3057. PubMed: 21931334.
- Charbit AR, Akerman S, Holland PR, Goadsby PJ (2009) Neurons of the dopaminergic/caltonin gene-related peptide A11 cell group modulate neuronal firing in the trigeminocervical complex: an electrophysiological and immunohistochemical study. *J Neurosci* 29: 12532-12541. doi:10.1523/JNEUROSCI.2887-09.2009. PubMed: 19812328.
- Zimmermann M (1983) Ethical guidelines for investigations of experimental pain in conscious animals. *Pain* 16: 109-110. doi: 10.1016/0304-3959(83)90201-4. PubMed: 6877845.
- Paxinos G, Watson CW (2007) *The rat brain in stereotaxic coordinates*. 6th Edition. San Diego: Academic Press.
- Biag J, Huang Y, Gou L, Hintiryan H, Askarinam A et al. (2012) Cyto- and chemoarchitecture of the hypothalamic paraventricular nucleus in the C57BL/6J male mouse: a study of immunostaining and multiple fluorescent tract tracing. *J Comp Neurol* 520: 6-33. doi:10.1002/cne.22698. PubMed: 21674499.
- Swanson LW, Kuypers HG (1980b) The paraventricular nucleus of the hypothalamus: cytoarchitectonic subdivisions and organization of projections to the pituitary, dorsal vagal complex, and spinal cord as demonstrated by retrograde fluorescence double-labeling methods. *J*

- Comp Neurol 194: 555-570. doi:10.1002/cne.901940306. PubMed: 7451682.
29. Cechetto DF, Saper CB (1988) Neurochemical organization of the hypothalamic projection to the spinal cord in the rat. *J Comp Neurol* 272: 579-604. doi:10.1002/cne.902720410. PubMed: 2901438.
  30. Nylén A, Skagerberg G, Alm P, Larsson B, Holmqvist B et al. (2001) Nitric oxide synthase in the hypothalamic paraventricular nucleus of the female rat; organization of spinal projections and coexistence with oxytocin or vasopressin. *Brain Res* 908: 10-24. doi:10.1016/S0006-8993(01)02539-2. PubMed: 11457427.
  31. Strassman AM, Vos BP (1993) Somatotopic and laminar organization of fos-like immunoreactivity in the medullary and upper cervical dorsal horn induced by noxious facial stimulation in the rat. *J Comp Neurol* 331: 495-516. doi:10.1002/cne.903310406. PubMed: 8509507.
  32. Molander C, Xu Q, Rivero-Melian C, Grant G (1989) Cytoarchitectonic organization of the spinal cord in the rat: II. The cervical and upper thoracic cord. *J Comp Neurol* 289: 375-385. doi:10.1002/cne.902890303. PubMed: 2808773.
  33. Yoshida A, Dostrovsky JO, Sessle BJ, Chiang CY (1991) Trigeminal projections to the nucleus submedialis of the thalamus in the rat. *J Comp Neurol* 307: 609-625. doi:10.1002/cne.903070408. PubMed: 1714465.
  34. Skagerberg G, Lindvall O (1985) Organization of diencephalic dopamine neurones projecting to the spinal cord in the rat. *Brain Res* 342: 340-351. doi:10.1016/0006-8993(85)91134-5. PubMed: 4041835.
  35. Swanson LW, Sanchez-Watts G, Watts AG (2005) Comparison of melanin-concentrating hormone and hypocretin/orexin mRNA expression patterns in a new parceling scheme of the lateral hypothalamic zone. *Neurosci Lett* 387: 80-84. doi:10.1016/j.neulet.2005.06.066. PubMed: 16084021.
  36. Swanson LW, Sawchenko PE (1983) Hypothalamic integration: organization of the paraventricular and supraoptic nuclei. *Annu Rev Neurosci* 6: 269-324. doi:10.1146/annurev.ne.06.030183.001413. PubMed: 6132586.
  37. Swanson LW, McKellar S (1979) The distribution of oxytocin- and neurophysin-stained fibers in the spinal cord of the rat and monkey. *J Comp Neurol* 188: 87-106. doi:10.1002/cne.901880108. PubMed: 115910.
  38. Saper CB, Loewy AD, Swanson LW, Cowan WM (1976) Direct hypothalamo-autonomic connections. *Brain Res* 117: 305-312. doi:10.1016/0006-8993(76)90738-1. PubMed: 62600.
  39. Schmued LC, Heimer L (1990) Iontophoretic injection of fluoro-gold and other fluorescent tracers. *J Histochem Cytochem* 38: 721-723. doi:10.1177/38.5.2332627. PubMed: 2332627.
  40. Dado RJ, Burstein R, Cliffer KD, Giesler GJ Jr (1990) Evidence that Fluoro-Gold can be transported avidly through fibers of passage. *Brain Res* 533: 329-333. doi:10.1016/0006-8993(90)91358-N. PubMed: 1705157.
  41. Köbber C, Apps R, Bechmann I, Lanciego JL, Mey J et al. (2000) Current concepts in neuroanatomical tracing. *Prog Neurobiol* 62: 327-351. doi:10.1016/S0301-0082(00)00019-8. PubMed: 10856608.
  42. Hosoya Y (1980) The distribution of spinal projection neurons in the hypothalamus of the rat, studied with the HRP method. *Exp Brain Res* 40: 79-87. PubMed: 7418761.
  43. Swanson LW, Kuypers HG (1980) A direct projection from the ventromedial nucleus and retrochiasmatic area of the hypothalamus to the medulla and spinal cord of the rat. *Neurosci Lett* 17: 307-312. doi:10.1016/0304-3940(80)90041-5. PubMed: 7052476.
  44. Sawchenko PE, Swanson LW (1982) Immunohistochemical identification of neurons in the paraventricular nucleus of the hypothalamus that project to the medulla or to the spinal cord in the rat. *J Comp Neurol* 205: 260-272. doi:10.1002/cne.902050306. PubMed: 6122696.
  45. Hosoya Y, Matsushita M (1979) Identification and distribution of the spinal and hypophyseal projection neurons in the paraventricular nucleus of the rat. A light and electron microscopic study with the horseradish peroxidase method. *Exp Brain Res* 35: 315-331. PubMed: 86456.
  46. Shaffon AD, Ryan A, Badoer E (1998) Neurons in the hypothalamic paraventricular nucleus send collaterals to the spinal cord and to the rostral ventrolateral medulla in the rat. *Brain Res* 801: 239-243. doi:10.1016/S0006-8993(98)00587-3. PubMed: 9729407.
  47. Wagner CK, Sisk CL, Clemens LG (1993) Neurons in the paraventricular nucleus of the hypothalamus that project to the sexually dimorphic lower lumbar spinal cord concentrate 3H-estradiol in the male rat. *J Neuroendocrinol* 5: 545-551. doi:10.1111/j.1365-2826.1993.tb00520.x. PubMed: 8680423.
  48. Nilaver G, Zimmerman EA, Wilkins J, Michaels J, Hoffman D et al. (1980) Magnocellular hypothalamic projections to the lower brain stem and spinal cord of the rat. Immunocytochemical evidence for predominance of the oxytocin-neurophysin system compared to the vasopressin-neurophysin system. *Neuroendocrinology* 30: 150-158. doi:10.1159/000122991. PubMed: 6154267.
  49. Portillo F, Carrasco M, Vallo JJ (1998) Separate populations of neurons within the paraventricular hypothalamic nucleus of the rat project to vagal and thoracic autonomic preganglionic levels and express c-Fos protein induced by lithium chloride. *J Chem Neuroanat* 14: 95-102. doi:10.1016/S0891-0618(97)10022-9. PubMed: 9625354.
  50. Hosoya Y, Matsushita M (1981) Brainstem projections from the lateral hypothalamic area in the rat, as studied with autoradiography. *Neurosci Lett* 24: 111-116. doi:10.1016/0304-3940(81)90232-9. PubMed: 6166908.
  51. Ondo WG, He Y, Rajasekaran S, Le WD (2000) Clinical correlates of 6-hydroxydopamine injections into A11 dopaminergic neurons in rats: a possible model for restless legs syndrome. *Mov Disord* 15: 154-158. doi:10.1002/1531-8257(200001)15:1. PubMed: 10634257.
  52. Skagerberg G, Bjorklund A, Lindvall O, Schmidt RH (1982) Origin and termination of the diencephalo-spinal dopamine system in the rat. *Brain Res Bull* 9: 237-244. doi:10.1016/0361-9230(82)90136-8.
  53. Holstege JC, Van Dijken H, Buijs RM, Goedknegt H, Gosens T et al. (1996) Distribution of dopamine immunoreactivity in the rat, cat and monkey spinal cord. *J Comp Neurol* 376: 631-652. doi:10.1002/(SICI)1096-9861(19961223)376:4. PubMed: 8978475.
  54. Qu S, Ondo WG, Zhang X, Xie WJ, Pan TH et al. (2006) Projections of diencephalic dopamine neurons into the spinal cord in mice. *Exp Brain Res* 168: 152-156. doi:10.1007/s00221-005-0075-1. PubMed: 16044299.
  55. Pappas SS, Tiernan CT, Behrouz B, Jordan CL, Breedlove SM et al. (2010) Neonatal androgen-dependent sex differences in lumbar spinal cord dopamine concentrations and the number of A11 diencephalospinal dopamine neurons. *J Comp Neurol* 518: 2423-2436. PubMed: 20503420.
  56. Barraud Q, Obeid I, Aubert I, Barrière G, Contamin H et al. (2010) Neuroanatomical study of the A11 diencephalospinal pathway in the non-human primate. *PLOS ONE* 5: e13306. doi:10.1371/journal.pone.0013306. PubMed: 20967255.
  57. Pasquier DA, Tramezzani JH (1979) Afferent connections of the hypothalamic retrochiasmatic area in the rat. *Brain Res Bull* 4(6): 765-771. doi:10.1016/0361-9230(79)90010-8.
  58. Berk ML, Finkelstein JA (1981) An autoradiographic determination of the efferent projections of the supra-chiasmatic nucleus of the hypothalamus. *Brain Res* 226: 1-13. doi:10.1016/0006-8993(81)91079-9. PubMed: 7296282.
  59. Stephan FK, Berkley KJ, Moss RL (1981) Efferent connections of the rat supra-chiasmatic nucleus. *Neuroscience* 6: 2625-2641. doi:10.1016/0306-4522(81)90108-1. PubMed: 7322354.
  60. Watts AG, Swanson LW (1987) Efferent projections of the supra-chiasmatic nucleus: II. Studies using retrograde transport of fluorescent dyes and simultaneous peptide immunohistochemistry in the rat. *J Comp Neurol* 258: 230-252. doi:10.1002/cne.902580205. PubMed: 2438309.
  61. Johnson RF, Morin LP, Moore RY (1988) Retinohypothalamic projections in the hamster and rat demonstrated using cholera toxin. *Brain Res* 462: 301-312. doi:10.1016/0006-8993(88)90558-6. PubMed: 3191391.
  62. Levine JD, Weiss ML, Rosenwasser AM, Miselis RR (1991) Retinohypothalamic tract in the female albino rat: a study using horseradish peroxidase conjugated to cholera toxin. *J Comp Neurol* 306: 344-360. doi:10.1002/cne.903060210. PubMed: 1711060.
  63. Morin LP, Goodless-Sanchez N, Smale L, Moore RY (1994) Projections of the supra-chiasmatic nuclei, subparaventricular zone and retrochiasmatic area in the golden hamster. *Neuroscience* 61: 391-410. doi:10.1016/0306-4522(94)90240-2. PubMed: 7526267.
  64. Card JP, Moore RY (1989) Organization of lateral geniculate-hypothalamic connections in the rat. *J Comp Neurol* 284: 135-147. doi:10.1002/cne.902840110. PubMed: 2754028.
  65. Elias CF, Saper CB, Maratos-Flier E, Tritos NA, Lee C et al. (1998) Chemically defined projections linking the mediobasal hypothalamus and the lateral hypothalamic area. *J Comp Neurol* 402: 442-459. doi:10.1002/(SICI)1096-9861(19981228)402:4. PubMed: 9862320.
  66. Meng ID, Hu JW, Benetti AP, Bereiter DA (1997) Encoding of corneal input in two distinct regions of the spinal trigeminal nucleus in the rat: cutaneous receptive field properties, responses to thermal and chemical stimulation, modulation by diffuse noxious inhibitory controls, and projections to the parabrachial area. *J Neurophysiol* 77: 43-56. PubMed: 9120584.
  67. Broton JG, Hu JW, Sessle BJ (1988) Effects of temporomandibular joint stimulation on nociceptive and nonnociceptive neurons of the cat's

- trigeminal subnucleus caudalis (medullary dorsal horn). *J Neurophysiol* 59: 1575-1589. PubMed: 3385474.
68. Hu JW (1990) Response properties of nociceptive and non-nociceptive neurons in the rat's trigeminal subnucleus caudalis (medullary dorsal horn) related to cutaneous and deep craniofacial afferent stimulation and modulation by diffuse noxious inhibitory controls. *Pain* 41: 331-345. doi:10.1016/0304-3959(90)90010-B. PubMed: 2388770.
  69. Raboisson P, Dallel R, Clavelou P, Sessle BJ, Woda A (1995) Effects of subcutaneous formalin on the activity of trigeminal brain stem nociceptive neurones in the rat. *J Neurophysiol* 73: 496-505. PubMed: 7760113.
  70. Burstein R, Yamamura H, Malick A, Strassman AM (1998) Chemical stimulation of the intracranial dura induces enhanced responses to facial stimulation in brain stem trigeminal neurons. *J Neurophysiol* 79: 964-982. PubMed: 9463456.
  71. Truedell LS, Bodnar RJ (1987) Reduction in cold-water swim analgesia following hypothalamic paraventricular nucleus lesions. *Physiol Behav* 39: 727-731. doi:10.1016/0031-9384(87)90257-5. PubMed: 3602125.
  72. Wang QA, Mao LM, Han JS (1990) Analgesia from electrical stimulation of the hypothalamic arcuate nucleus in pentobarbital-anesthetized rats. *Brain Res* 526: 221-227. doi: 10.1016/0006-8993(90)91225-6. PubMed: 2257483.
  73. Yirmiya R, Ben-Eliyahu S, Shavit Y, Marek P, Liebeskind JC (1990) Stimulation of the hypothalamic paraventricular nucleus produces analgesia not mediated by vasopressin or endogenous opioids. *Brain Res* 537: 169-174. doi:10.1016/0006-8993(90)90354-E. PubMed: 1982239.
  74. Miranda-Cardenas Y, Rojas-Piloni G, Martínez-Lorenzana G, Rodríguez-Jiménez J, López-Hidalgo M et al. (2006) Oxytocin and electrical stimulation of the paraventricular hypothalamic nucleus produce antinociceptive effects that are reversed by an oxytocin antagonist. *Pain* 122: 182-189. doi:10.1016/j.pain.2006.01.029. PubMed: 16527400.
  75. Yang J, Chen JM, Song CY, Liu WY, Wang G et al. (2006) Through the central V2, not V1 receptors influencing the endogenous opiate peptide system, arginine vasopressin, not oxytocin in the hypothalamic paraventricular nucleus involves in the antinociception in the rat. *Brain Res* 1069: 127-138. doi:10.1016/j.brainres.2005.11.045. PubMed: 16409991.
  76. Pinto-Ribeiro F, Ansah OB, Almeida A, Pertovaara A (2008) Influence of arthritis on descending modulation of nociception from the paraventricular nucleus of the hypothalamus. *Brain Res* 1197: 63-75. doi:10.1016/j.brainres.2007.12.038. PubMed: 18242585.
  77. Matsumoto N, Kawarada K, Kamata K, Suzuki TA (1993) Electrical stimulation of tooth pulp increases the expression of c-fos in the cat supraoptic nucleus but not in the paraventricular nucleus. *Life Sci* 53: 1235-1241. doi:10.1016/0024-3205(93)90542-B. PubMed: 8412481.
  78. Berkowitz BA, Sherman S (1982) Characterization of vasopressin analgesia. *J Pharmacol Exp Ther* 220: 329-334. PubMed: 7057394.
  79. Breton JD, Veinante P, Uhl-Bronner S, Vergnano AM, Freund-Mercier MJ et al. (2008) Oxytocin-induced antinociception in the spinal cord is mediated by a subpopulation of glutamatergic neurons in lamina I-II which amplify GABAergic inhibition. *Mol Pain* 4: 19. doi: 10.1186/1744-8069-4-19. PubMed: 18510735.
  80. Mogil JS, Sorge RE, LaCroix-Fralish ML, Smith SB, Fortin A et al. (2011) Pain sensitivity and vasopressin analgesia are mediated by a gene-sex-environment interaction. *Nat Neurosci* 14: 1569-1573. doi: 10.1038/nn.2941. PubMed: 22019732.
  81. Zubrzycka M, Janecka A (2005) Effects of centrally administered vasopressin on orofacial pain perception in rats. *Brain Res* 1051: 112-116. doi:10.1016/j.brainres.2005.05.058. PubMed: 15993385.
  82. Zubrzycka M, Janecka A (2008) Interactions of galanin with endomorphin-2, vasopressin and oxytocin in nociceptive modulation of the trigemino-hypoglossal reflex in rats. *Physiol Res* 57: 769-776. PubMed: 17949254.
  83. Mazzuca M, Minlebaev M, Shakirzyanova A, Tyzio R, Taccola G et al. (2011) Newborn analgesia mediated by oxytocin during delivery. *Front Cell Neurosci* 5: 3. PubMed: 21519396.
  84. Gura EV (2000) Vasopressin-mediated modulation of trigeminal reflexes in rats. *Neurophysiology* 32: 371-375. doi:10.1023/A: 1010487932269.
  85. Franco AC, Prado WA (1996) Antinociceptive effects of stimulation of discrete sites in the rat hypothalamus: evidence for the participation of the lateral hypothalamus area in descending pain suppression mechanisms. *Braz J Med Biol Res* 29: 1531-1541. PubMed: 9196558.
  86. Dafny N, Dong WQ, Prieto-Gomez C, Reyes-Vazquez C, Stanford J et al. (1996) Lateral hypothalamus: site involved in pain modulation. *Neuroscience* 70: 449-460. doi:10.1016/0306-4522(95)00358-4. PubMed: 8848153.
  87. Peyron C, Tighe DK, van den Pol AN, De Lecea L, Heller HC et al. (1998) Neurons containing hypocretin (orexin) project to multiple neuronal systems. *J Neurosci* 18: 9996-10015. PubMed: 9822755.
  88. van den Pol AN (1999) Hypothalamic hypocretin (orexin): robust innervation of the spinal cord. *J Neurosci* 19: 3171-3182. PubMed: 10191330.
  89. Sakurai T, Mieda M (2011) Connectomics of orexin-producing neurons: interface of systems of emotion, energy homeostasis and arousal. *Trends Pharmacol Sci* 32: 451-462. doi:10.1016/j.tips.2011.03.007. PubMed: 21565412.
  90. Chiou LC, Lee HJ, Ho YC, Chen SP, Liao YY et al. (2010) Orexins/hypocretins: pain regulation and cellular actions. *Curr Pharm Des* 16: 3089-3100. doi:10.2174/138161210793292483. PubMed: 20687883.
  91. Holland PR, Akerman S, Goadsby PJ (2006) Modulation of nociceptive dural input to the trigeminal nucleus caudalis via activation of the orexin 1 receptor in the rat. *Eur J Neurosci* 24: 2825-2833. doi:10.1111/j.1460-9568.2006.05168.x. PubMed: 17156207.
  92. Rainero I, Rubino E, Gallone S, Fenoglio P, Picci LR et al. (2011) Evidence for an association between migraine and the hypocretin receptor 1 gene. *J Headache Pain* 12: 193-199. doi:10.1007/s10194-011-0314-8. PubMed: 21344296.
  93. Fleetwood-Walker SM, Hope PJ, Mitchell R (1988) Antinociceptive actions of descending dopaminergic tracts on cat and rat dorsal horn somatosensory neurones. *J Physiol* 399: 335-348. PubMed: 2841456.
  94. Wei H, Viisanen H, Pertovaara A (2009) Descending modulation of neuropathic hypersensitivity by dopamine D2 receptors in or adjacent to the hypothalamic A11 cell group. *Pharmacol Res* 59: 355-363. doi: 10.1016/j.phrs.2009.01.001. PubMed: 19416636.
  95. Taniguchi W, Nakatsuka T, Miyazaki N, Yamada H, Takeda D et al. (2011) In vivo patch-clamp analysis of dopaminergic antinociceptive actions on substantia gelatinosa neurons in the spinal cord. *Pain* 152: 95-105. doi:10.1016/j.pain.2010.09.034. PubMed: 21050660.
  96. Lapirot O, Melin C, Modolo A, Nicolas C, Messaoudi Y et al. (2011) Tonic and phasic descending dopaminergic controls of nociceptive transmission in the medullary dorsal horn. *Pain* 152: 1821-1831. doi: 10.1016/j.pain.2011.03.030. PubMed: 21514054.
  97. Bellasio S, Nicolussi E, Bertorelli R, Reggiani A (2003) Melanocortin receptor agonists and antagonists modulate nociceptive sensitivity in the mouse formalin test. *Eur J Pharmacol* 482: 127-132. doi:10.1016/j.ejphar.2003.09.017. PubMed: 14660013.
  98. Peterlin BL, Rapoport AM, Kurth T (2010) Migraine and obesity: epidemiology, mechanisms, and implications. *Headache* 50: 631-648. doi:10.1111/j.1526-4610.2009.01554.x. PubMed: 19845784.